CHAPTER VI
THERMAL AND MECHANICAL PROPERTIES OF PP/ORGANOCLAY NANOCOMPOSITES

6.1 Abstract

The modification of clay by ion exchange reaction with cationic surfactants plays an important role in the greater interlayer spacing of Na-bentonite. The cationic surfactant, Dipalmitoylethy Hydroxyethylmonium Methosulfate under trade name STPANTEX^{TM} SP-90, was introduced into the clay in order to investigate the effects of intercalation of the cationic surfactants. The organobentonites were characterized by XRD, FTIR and TGA. Polypropylene and the organoclay were melted compounding through a twin screw extruder using Surlyn® as a reactive compatibilizer by varying the clay contents 1, 3, and 5wt%. Subsequently, the nanoclay composites were determined thermal behavior, crystallization behavior, mechanical properties, and gas permeability.

6.2 Introduction

The development of organic-inorganic nanoscale composites have attracted a great deal of interest from researchers, both in industry and in academia, because they often exhibit superior hybrid properties that are synergistically derived from the two components. One of the most promising of the composites are polymer-clay nanocomposites, which have superior physical and mechanical properties, even at low clay content by comparison with more conventional polymer-microcomposites.

In recent studies, polypropylene (PP) /clay hybrids have attracted great research interest because clay nanocomposites can produce dramatic improvements in a variety of properties. [1] Moreover, PP is one of the most widely used polymers. It shows a very positive combination of properties, including high stiffness, as well as good thermal and chemical resistance, as compared to other thermoplastics of similar price. However, PP is a non-polar polymer incompatible with polar-clay and is consequently difficult to get the exfoliated and homogeneous dispersion of the clay par-

ticles at the nanometer level in the polymer. Among the many properties that are modified, the observed mechanical properties and compatibility between non-polar PP and silicate layers are poor. To overcome this problem, modifying the surface polarity of the clay, alkylammonium ions allow thermodynamically favourable penetration of polymer into the interlayer region. The ability of the alkylammonium ions to assist in delaminating of the clay depends on its chemical nature such as its polarity. The loading of the alkylammonium ion on the clay is also important.

The clay is naturally a hydrophilic material, which makes it difficult to exfloliate in a non-polar polymer matrix. Therefore, the surface treatment of silicate layers is necessary to render its surface more hydrophobic, which facilitates exfoliation. Generally, this can be done by ion exchange reaction with cationic surfactants. This modification also leads to expand the basal spacing between the silicate layers due to the presence of alkyl chain intercalated in the interlayer. However, in the case of polypropylene, it is frequently necessary to use a compatibilizer such as ethylene methacrylic acid copolymer, Surlyn®. There are two important factors to achieve the exfoliation of the clay layer silicates: (1) the compatibilizer should be miscible with polymer matrix, and (2) it should include a certain amount of polar functional groups in a molecule. Surlyn® can fulfill the two requirements and is frequently used as a compatibilizer for polypropylene nanocomposites. [2, 3, 4]

The aim of this study is to determine the effect of organoclay content in the system of polypropylene/organoclay on the thermal behavior, crystallization behavior, mechanical properties, and gas permeability. The polypropylene/organoclay composites were prepared by two-step compounding method using Surlyn® as a reactive compatibilizer through a twin screw extruder. The state of dispersion was analyzed by X-ray diffraction and the influence of this filler on thermal and mechanical properties was examined.

6.3 Experimental

A. Preparation of organomodified bentonite

350 g of Na-bentonite, (Mac-Gel® GRADE SAC) supplied by Thai Nippon Co., Ltd. Thailand, was swollen in water 1.05 liter for 24 hr. STPANTEX™ SP-90

as an alkyl ammonium ion (2.0CEC) was dissolved in 100 ml of ethanol. The whole swollen clay was then mixed with cationic surfactant solution with vigorous stirring for 2-3 hr at 80°C. After that the sediment was filtrated and washed with hot water several times to remove to excess salts. It was dried in a vacuum oven at 100°C overnight and ground before being screened through a mesh #325.

B. Preparation of PP/clay nanocomposites

The master batches containing 50 wt% organomodified clays with a compatibilizer were initially prepared using a Model T-20 co-rotating twin-screw extruder (Collin) with L/D=30 and D=25 mm. The operating temperatures of extruder were performed at 80, 170, 180, 190, 200, and 210°C from hopper to die, respectively, with 50 rpm of screw speed.

The master batch was then added to PP in appropriate amounts to obtain nominal contents of 1, 3 and 5 wt% clays in the nanocomposites. In this preparation, the compatibilizer was fixed at 6 wt%. Each composition was dried in a vacuum oven at 80°C for 12 h for moisture removal and then premixed by a tumble mixer for 10 min before introducing into the twin-screw extruder by Collin D-8017 T20 twin screw extruder with L/D ratio of 30 and 25-mm-diameter. The operating temperatures were maintained at 80/160/180/190/200/210°C from feed to die with screw speed of 50 rpm to yield strands of the nanocomposites. Then, the extruded thick strand was quenched immediately in water, and pelletized.

PP/organoclay nanocomposites films were prepared by blown film extrusion machine at Tang Packaging Co., Ltd. The screw speed was 50 rpm, screw diameter was 45mm, L/D was 26 and the processing temperature was 210°C. Finally, molded samples were immediately sealed in a plastic bag and placed in a vacuum desiccator for a minimum of 24 h prior to material property evaluation.

C. Characterizations

Fourier transform infrared spectroscopy (FT-IR) was used to investigate the presence of the cationic surfactant. The FT-IR spectra were recorded using a Nicolet Nexus 670 FT-IR spectrometer in the frequency range of 4000-400 cm^{-1} with 32 scans at a resolution of 2 cm^{-1}.

The structure of organobentonite and its nanocomposites in PP was analyzed by wide angle X-ray diffraction (WAXD) using a Rigaku Model Dmax 2002 diffractometer with Ni-filtered Cu K_α radiation operated at 40 kV and 30 mA. The experiment was performed in the 2θ range of 2-20 degrees with scan speed 2 degree/min and scan step 0.01 degree. The crystal structures of PP/organoclay nanocomposites were also analyzed by Wide angle X-ray diffraction (WAXD) using a Rigaku Model Dmax 2002 performed in the 2θ range of 2-40 degrees with the same scan speed and scan step as performed in organoclays.

Thermogravimetric analysis (TGA) was used to study thermal stability of organomodified bentonite and PP/organoclay nanocomposites as compared to the pure PP. DTA curves-TG, cted on acolle Perkin-Elmer Pyris Diamond TG/DTA instrument. The degradation temperature, initial degradation temperature, weight loss, and final degradation temperature of the samples were determined. The nanocomposite pellets from twin screw extruder as well as PP pellets were loaded on platinum pan and heated from 30°C to 90°C at heating rate 10°C/min and flow under N_2 200 ml/min.

The crystallization and melting behaviors of the PP/organoclay nanocomposites were measured with a Perkin-Elmer DSC 7 analyzer. All operations were performed under a nitrogen atmosphere. The samples were first heated from 30°C to 200°C at a heating rate of 10°C/min in order to eliminate the influence of thermal history and then cooled down at a rate of 10°C/min from 200°C to 30°C to observe the melt crystallization behavior. After that the sample was immediately reheated to 200°C at the same heating rate in order to observe the melting behavior. The crystallinity can be calculated with the following formula

$$\% \text{ crystallinity} = \frac{\Delta H_{sample}}{\Delta H^{0}_{PP}} \times 100$$

ΔH = enthalpy of fusion of the sample (J/g)

ΔH = enthalpy of fusion of completely crystalline PP (~ 209 J/g)

The dispersion of organomodified bentonite in polymer matrix was determined by using SEM (JEOL/JEM 5800 LV). The selected samples were dipped and

fractured in liquid nitrogen. Then the samples were sputtered with gold before viewing under a scanning electron microscope (SEM) operating at 15 kV.

The mechanical properties tests were conducted according to ASTM D882 using Lloyd universal testing machine equipped with an extensometer. The blown film specimen was cut in machine direction into rectangular shape with 10x100 mm. The tests were operated at a crosshead speed of 50 mm/min. The data was recorded at room temperature without preconditioning of the samples. The mean values were obtained from at least 5 separated tests.

Gas permeability tester, Oxygen Permeation Analyzer Model 8000, Illinois Instrument Inc., was used to determine oxygen permeability constants of pristine PP and nanocomposite films. Gas permeation experiments were investigated following the procedure described in ASTM D1434. The condition was proceed at 23 °C with oxygen flow rate is 50 cm^2/min. The films were prepared from a compression-molded sheet with the same thickness of 150 μm and were cut into circular shape with 15 cm in diameter. The thickness of the films was measured by using the peacock digital thickness gauge model PDN 12N by reading 15 points at random position over tested area and the results were averaged.

6.4 Results and Discussion

A. Characterizations of the organomobentonite

In this research work attempts to incorporate food sensors onto a nanocomposite polymer films were carried out. Prior to study the characteristics of the food sensors, characteristic of the nanocomposite films were conducted.

The clay samples sodium bentonite (Na-BTN) and organo-bentonite (OBTN) were analyzed by FTIR, XRD and TGA to confirm the organophilic nature after modification. From FTIR results (Figure 6.1) it is clear that the OBTN showed new absorptions bands at 2921 and 2852 cm^{-1} (assigned to symmetric and asymmetric stretching of CH_3, respectively) and at 1740 cm^{-1} (due to stretching vibrations of C=O). These results indicate that the salt molecules were incorporated into the clay structure. [5]

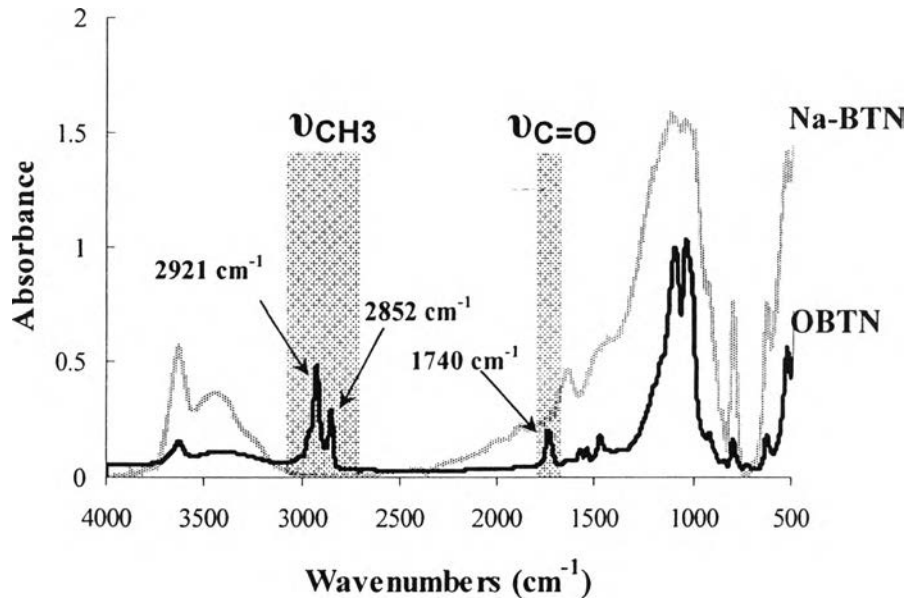

Figure 6.1 FTIR spectra of (a) Na-BTN and (b) OBTN.

With the cation exchange of the sodium ion for the cationic surfactant, Di-palmitoylethy Hydroxyethylmonium Methosulfate expansion of the Na-BTN clay layers occurs. This expansion was readily measure by X-ray diffraction (XRD). Figure 6.2 shows XRD profiles of Na-BTN and OBTN. The peaks correspond to the (001) reflections of the clay. The d_{001} peak of pristine BTN at $2\theta = 7.62°$ which corresponds to 1.15 nm (Figure 6.2 a) interlayer spacing. OBTN shows the d_{001} at 5.92° and 4.42° which corresponds to basal spacing of 1.49 and 1.99 nm, respectively (Figure 6.2 b). The d_{001} peak of OBTN (Figure 6.2 b) is observed at lower angle than that of pristine BTN; these indicate the ammonium ions intercalated into the silicate layers and expanded the basal spacing. [6] However, OBTN shows broad peaks at lower angles. This may imply that the inhomogeneous distribution of surfactant between layers of clay. [3]

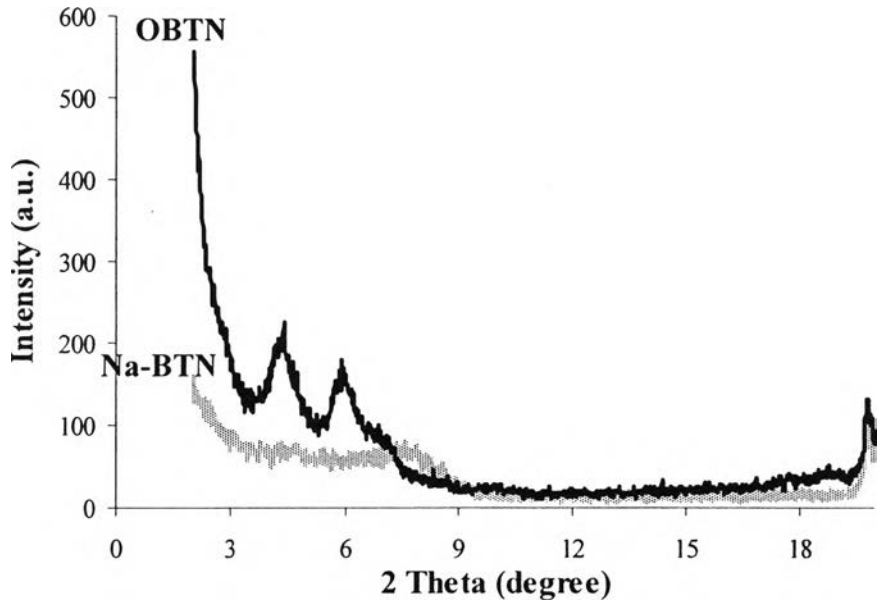

Figure 6.2 The XRD patterns: (a) BTN and (b) OBTN

Table 6.1 Thermal behavior of BTN and OBTN.

Sample	Mass Loss H_2O (wt%)	Mass Surfactant (wt%)	Char Residual (wt%)	Desurfactant		
				T_d (°C)	T_i (°C)	T_f (°C)
BTN	0.52	-	98.33	-	-	-
OBTN	0	35.4	64.3	336.8	270.8	367.8

Results from thermogravimetric analysis (TGA) of Na-BTN and OBTN are depicted in Table 6.1. For Na-BTN, decomposition at 654.2°C about 1.14 % mass losses associated with dehydroxylation of the aluminosilicate was observed. On the OBTN the mass losses of surfactant was shown at temperature range of 270-370°C, which was related to the thermal decomposition of OBTN, derived from the decomposition of the intercalated cationic surfactants within the clay interlayer. [7, 8] Hence, confirming the effectiveness of the procedure, as already observed by FTIR and XRD.

B. Thermal behavior of PP/organoclay nanocomposites

The melting and crystallization behavior, as measured by DSC. Differential scanning calorimeter thermograms of polymer/organoclay nanocomposites with various clay contents are shown in Figure 6.3 and Table 6.2. With increasing clay content, Melting temperature of the composite closed to virgin PP. However, the crystallization temperature of polymer/organoclay nanocomposite is thought to increase and the crystallinities of the nanocomposites are higher than that of pure PP but less sensitive to the clay content (1, 3, 5 wt%). This could be attributed to the OBTN acting as the nucleating agent for crystallization of PP. [9]

Table 6.2 Melting and crystallization behavior of PP and PP/organoclay nanocomposite films

Sample	$T_{c, peak}$ (°C)	$T_{m, peak}$ (°C)	ΔH_m (J/g)	% crystallinity
PP	108.63	158.37	69.46	33.23
PP/6%Surlyn	113.3	159.7	73.46	33.15
PP/6%Surlyn/1%Clay	109.97	159.2	66.10	32.10
PP/6%Surlyn/3%Clay	110.3	158.87	64.61	31.87
PP/6%Surlyn/5%Clay	112.3	159.2	61.59	31.02

PP 100% Crystallinity, ΔH_m = 209 J/g

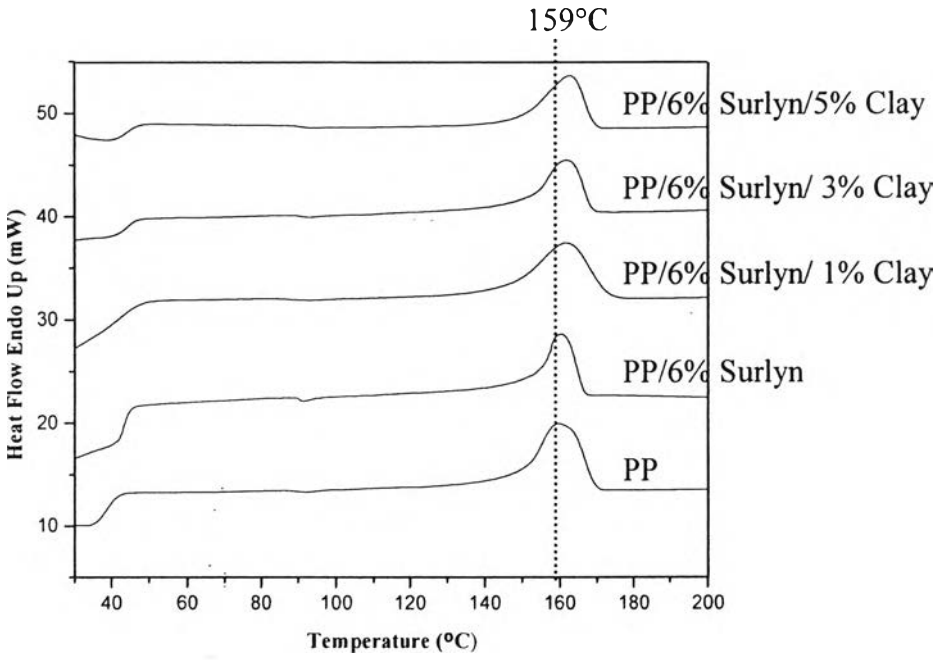

(A)

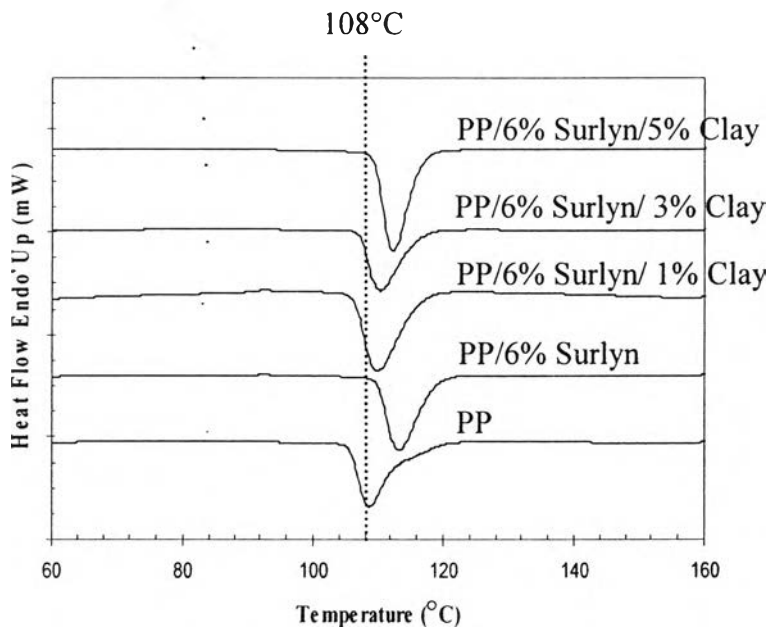

(B)

Figure 6.3 DSC thermograms of PP/organoclay nanocomposites film (A) Melting temperature, and (B) Crystallization temperature.

When thermal stability of the nanocomposite film was studied, it was found that the introduction of clay into PP enhances the thermal stability of PP, as shown in Table 6.3. This behavior may be attributed to the formation of a high-performance carbonaceous-silicate char on the surface of the nanocomposites, creating a physical protective barrier on the surface of the material. [7, 10]

Table 6.3 Thermal behavior of PP and PP/organoclay nanocomposite films

	TGA			
	Residue Content (wt%)	**T_d (°C)**	**T_i (°C)**	**T_f (°C)**
PP	-	443.7	420.5	453.7
PP/6%Surlyn	-	444.3	429.0	456.6
PP/6%Surlyn/1%Clay	6.7	445.7	428.4	455.3
PP/6%Surlyn/3%Clay	7.1	446.6	427.0	456.1
PP/6%Surlyn/5%Clay	11.3	447.6	427.2	457.1

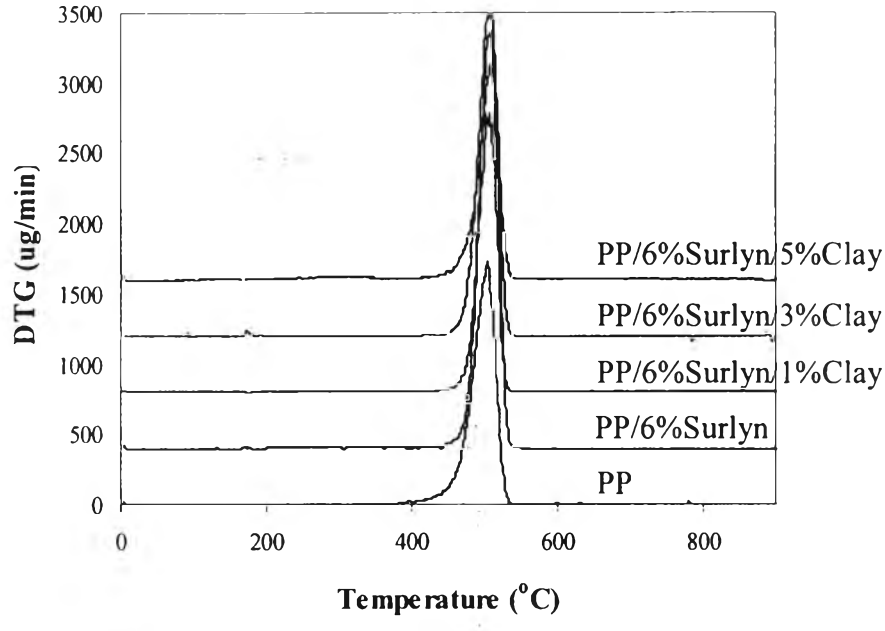

Figure 6.4 DTG curves of PP/organo-bentonite nanocomposite films.

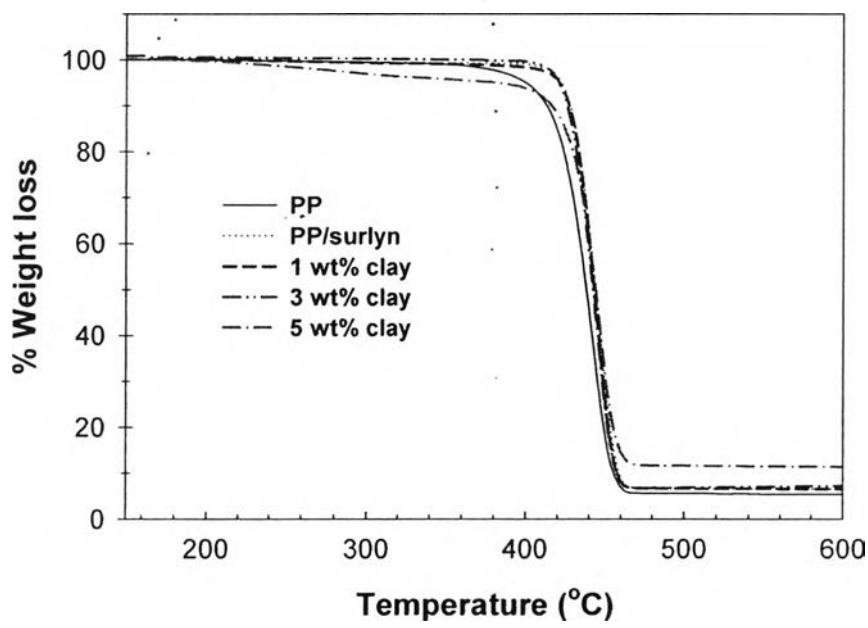

Figure 6.5 TG curves of PP/organo-bentonite nanocomposite films.

C. Crystallization behavior of PP/organoclay nanocomposites

The structure of the nanocomposites was examined by XRD. The characteristic peaks of PP crystal peak were analyzed with the 2θ range of 2-40°, as shown in Figore 6.6. According to the WAXD pattern, the (001) diffraction peaks of 3% and 5%clay in nanocomposite films presents at $2\theta = 5.88°$ and $2\theta = 5.72°$ which correspond to the interlayer spacing of 1.50 and 1.54 nm, respectively. Nevertheless, at 1%clay, the low angle peak was not observed. The silicate layers were delaminated and dispersed in the PP matrix. Therefore, exfoliated structure was achieved at 1%clay. Pristine PP shows five prominent which correspond to monoclinic α crystalline phase: α_1, α_2, α_3 and α_4 belong to the (110), (040), (130) and (111, 041) crystal plannar corresponding to 2θ = 14.04, 16.86, 18.50, 21.08, and 21.72, respectively. There is no obvious difference between them. It seems that the addition of OBTN does not affect the crystal structure of the PP matrix. [7, 10, 11]

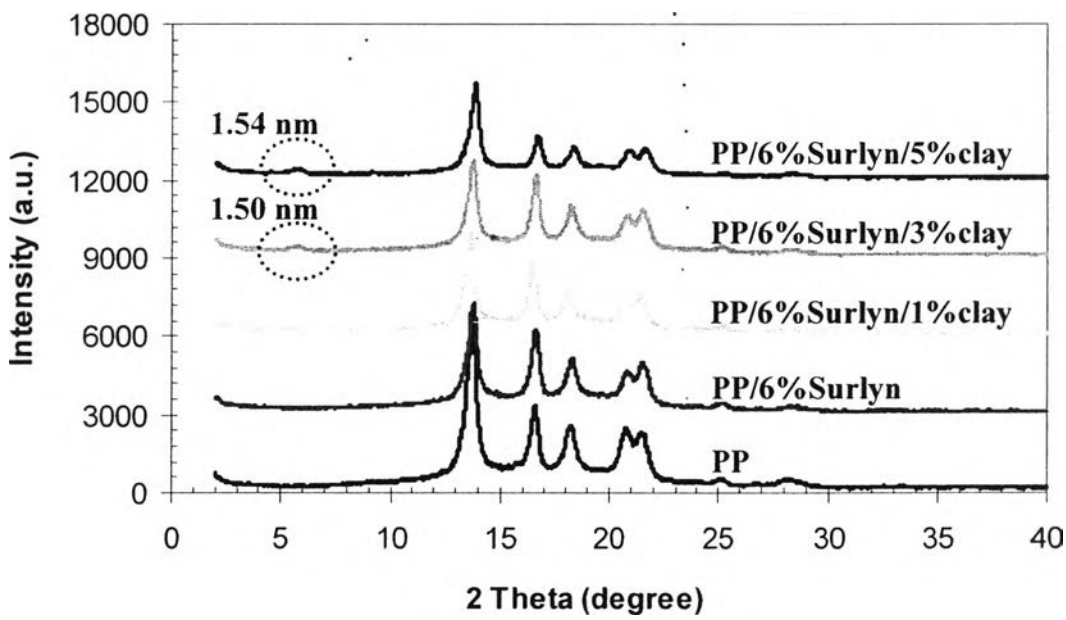

Figure 6.6 The WAXD patterns of pure PP and PP/organoclay composites varied the compositions.

D. Mechanical measurement of PP/organoclay nanocomposites

The influence of the organoclay content on the mechanical properties is shown in Figure 6.7, 6.8, and 6.9. The Young's modulus of films slightly increased to the hightest point at 1% organoclay is shown in Figure 6.7. However, when clay content is 5% wt, Young's modulus was decreased. Probably due to the aggregation of the organoclay, this leads to the loss of the features of the nanocomposites.

Moreover, the impurity of the bentonite is another important factor on stress at break as shown in Figure 6.8 and 6.9. Tensile strength and elongation at break slightly decrease with increasing percent of organoclay content. This occurrence could be explained that the modified bentonite has many inhomogeneous aggregates, calcium content and siliceous impurities. They act as stress concentrators, allowing crack initiation and propagation. [3] Additionally, the obstruction of organoclay to the movement of polypropylene matrix was another problem in decline of the elongation at break with increasing clay content which probably leads to lower polymeric chain mobility, making the material more rigid. [12]

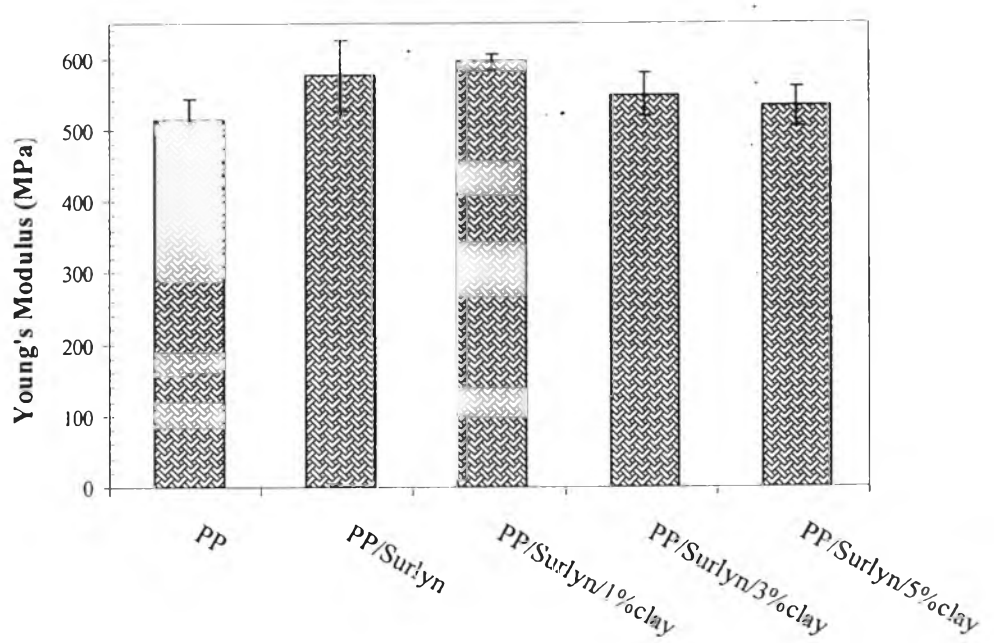

Figure 6.7 Young's modulus of PP and PP/organoclay composites with various organoclay loadings.

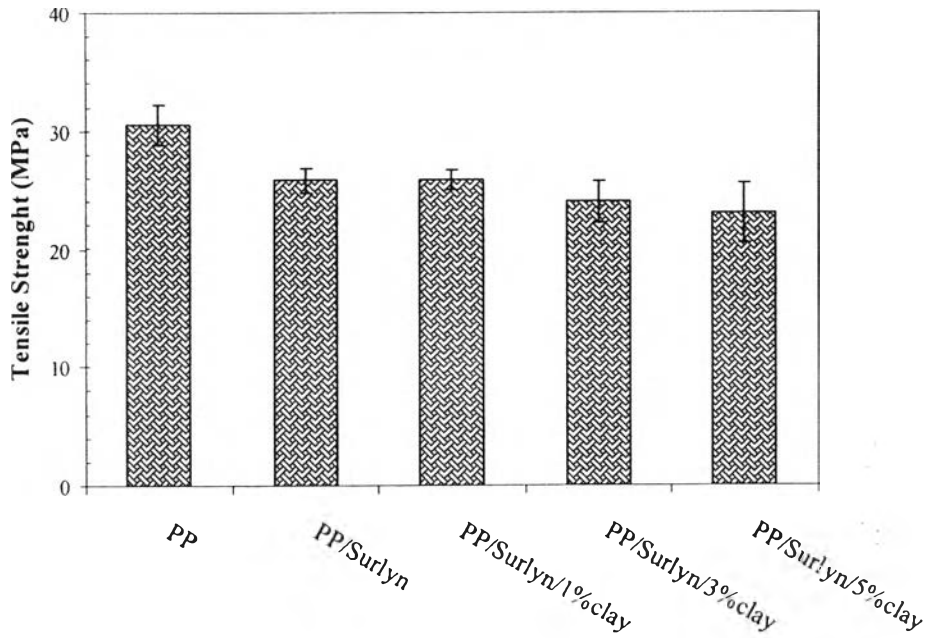

Figure 6.8 Tensile strength of PP and PP/organoclay composites with various organoclay loadings.

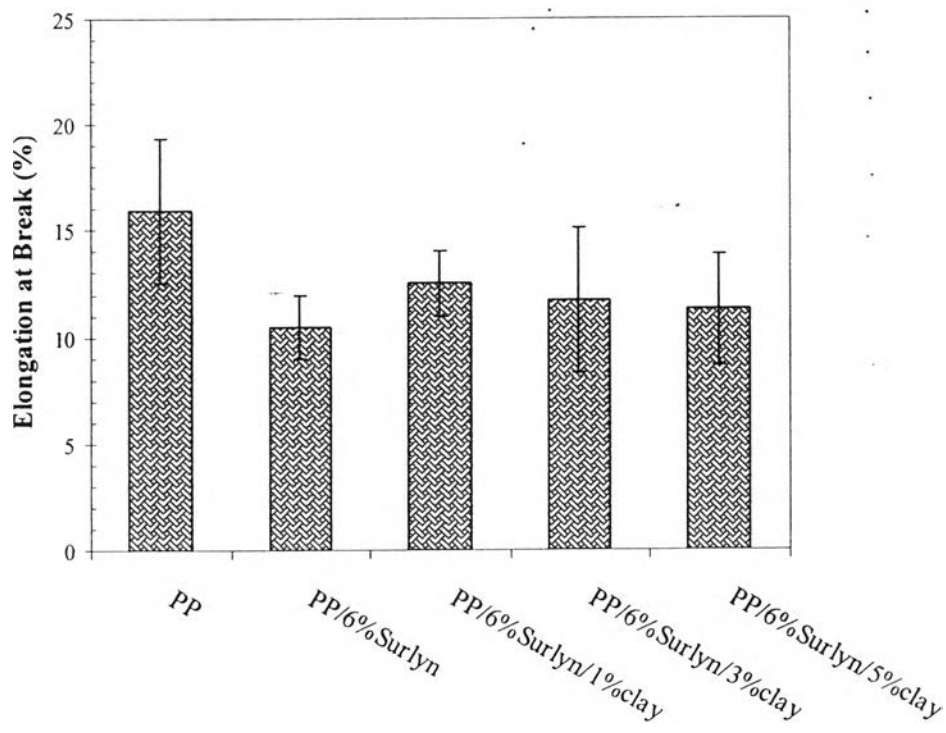

Figure 6.9 %Elongation at break of PP and PP/organoclay composites with various organoclay loadings.

E. Dispersion of OBTN in nanocomposite films

Figure 6.10 shows the SEM images of OBTN in nanocomposites films at different level. The figure implies that with increase of clay content, the aggregation of clay and its impurity in the PP matrix could be formed in films. The resulting of incompatibility between polymer matrix and clay also affect to the mechanical properties of films as mention prior. [13]

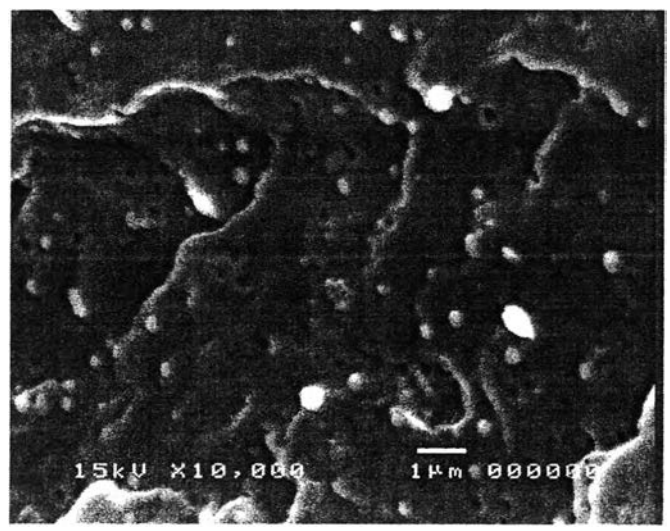

(A)

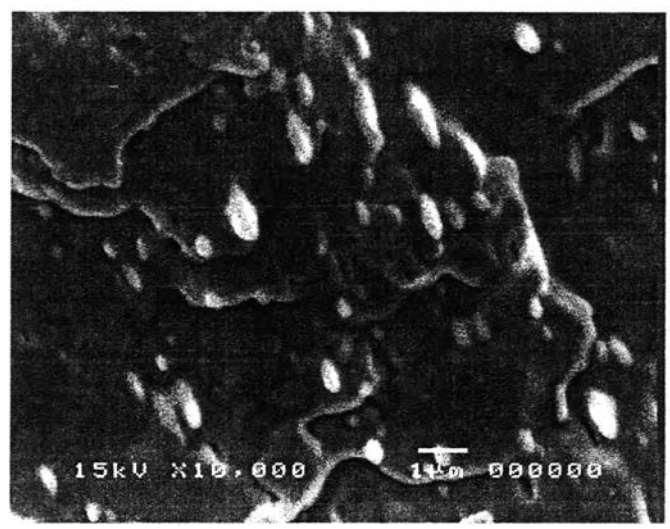

(B)

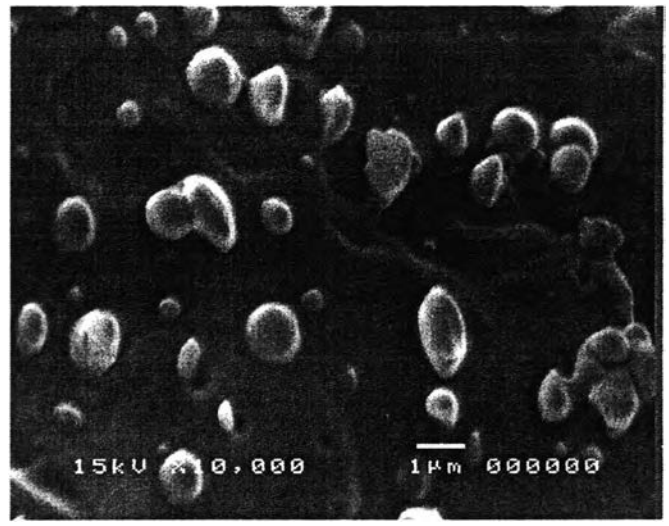

(C)

Figure 6.10 SEM images of nanocomposite films at 10000 magnification; (A) 1%wt organoclay, (B) 3%wt organoclay, (C) 5%wt organoclay.

F. Oxygen Gas Permeability of PP/OBTN Nanocomposite Films

The oxygen gas permeability of PP/OBTN nanocomposites films shows in Figure 6.11. The oxygen transitions rate of PP, PP/Surlyn, 1%wt clay, 3%wt clay, and 5%wt clay were 3580, 1649, 634, 627, and 615 cc/m^2/day, respectively. This reveals that amount of organoclay content affect to oxygen gas permeability. The reduction of oxygen gas permeability can be attributed to more tortuous path that retard the progress of gas molecules through the PP matrix, providing the improvement of gas barrier properties. [14, 15] Another possible explanation for the reduction in permeability is that crystalline act in a similar manner to crosslinking, restricting the motion of the chains involved in the diffusion process [16].

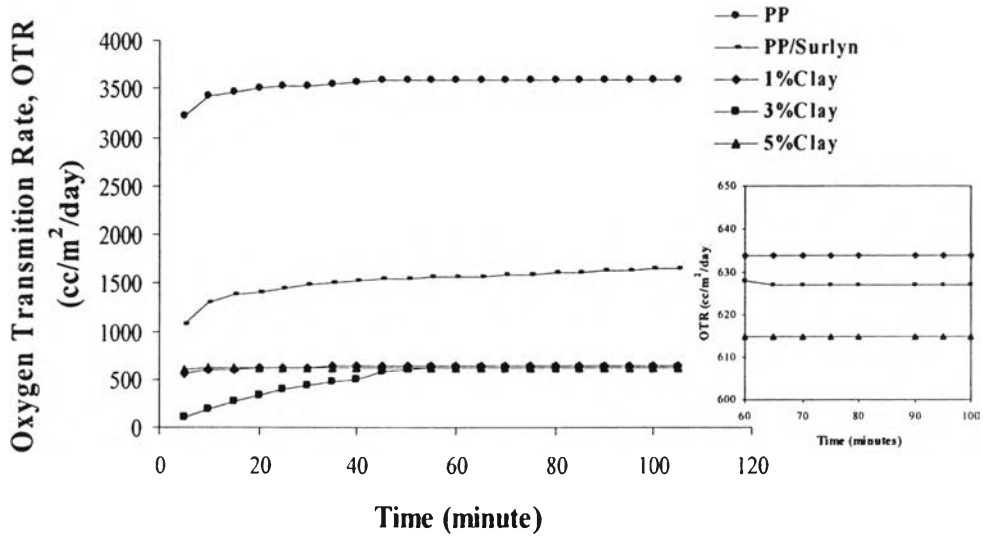

Figure 6.11 Oxygen transitions rate of PP and PP/OBTN nanocomposite films at different amount of clay content.

6.5 Conclusions

PP/organoclay nanocomposites with partial exfoliation of clay platelets should be achieved for 1% wt organoclay addition. The clay content has a direct influence on the mechanical properties of the obtained nanocomposites. The improvement is marked for the samples with 1 %wt of the organoclay with the highest Young's modulus, stress at break and %elongation at break. PP/organoclay composites start to drop in all mechanical properties when the organoclay is incorporated more than 1%wt. This resulting from the impurity of bentonite. They act as stress concentrators, allowing crack initiation and propagation to nanocomposite films. Moreover, information found in SEM image also confirms agglomeration of the organoclay and its impurity. However, a good point of increasing of clay content was the increasing of oxygen barrier properties. Clay obstructs diffusion of oxygen gas through the nanocomposite film, so oxygen gas permeability was reduced. The melting and crystallinity of nanocomposites were insignificantly changed however the thermal stability is better.

6.6 Acknowledgements

This work was funded by National Research Council of Thailand (NRCT). The author thanks for the Scholarship that is partially supported by the Petroleum and Petrochemical College; the National Excellence Center for Petroleum, Petrochemicals and Advanced Materials, Thailand; and Polymer Processing and Polymer Nanomaterial Research Units. The authors would like to thank Thai Nippon Chemical Industry Co, Ltd., for providing the raw materials to carry out this research and Tang Packaging Co., Ltd. for tubular blown film extrusion machine.

6.7 References

[1] Chiu, F.C., Lai, S.M., Chen, J.W., and Chu, P.S. (2004) Combined effects of clay modifications and compatibilizers on the formation and physical properties of melt-mixed polypropylene/clay nanocomposites. Polmer Science, 42, 4139-4150.

[2] Shah, R.K., Hunter, D.L., and Paul, D.R. (2005) Nanocomposites from poly(ethylene-co-methacrylic acid) ionomers: effect of surfactant structure on morphology and properties. Polymer, 46, 2646-2662.

[3] Garcia-Lopez, D., Picazo, O., Merino, J.C., and Pastor, J.M. (2003) Polypropylene-clay nanocomposites: effect of compatibilizing agents on clay dispersion. European Polymer, 39, 945-950.

[4] Lertwimolnun, W., and Vergnes, B. (2005) Influence of compatibilizer and processing conditions on the dispersion of nanoclay in a polypropylene matrix. Polymer, 46, 3462–3471.

[5] Choy, J., Kwak, S., Han, Y., and Kim, B. (1997) New organo-montmorillonite complexes with hydrophobic and hydrophilic functions. Materials Letters, 33, 143-147.

[6] Tang, Y., Hu, Y., Song, L., Zong, R., Gui, Z., Chen, Z., and Fan, W. (2003) Preparation and thermal stability of polypropylene/montmorillonite nanocomposites. Polymer Degradation and Stability, 82, 127–131.

[7] Ding, C., Jia, D., He, H., Guo, B., and Hong, H. (2004) How organo-montmorillonite truly affects the structure and properties of polypropylene. Polymer Testing, 24, 94-100.

[8] He, H., Duchet, J., Galy, J., and Gerard, J-F. (2005) Grafting of swelling clay materials with 3-aminopropyltriethoxysilane. Colloid and Interface Science, 288, 171-176.

[9] Maio, E., Iannace, S., Sorrentino, L., and Nicolais, L. (2004) Isothermal crystallization in PCL/clay nanocomposites investigated with thermal and rheometric methods. Polymer , 45, 8893-8900.

[10] Ramos, F.G., Melo, T.A., Rabello, M.S., and Silva, S.M. (2005) Thermal stability of nanocomposites based on polypropylene and bentonite. Polymer Degradation and Stability, 89, 383-392.

[11] Lai, S., Chen, J., and Chu, P. (2004) Combined effects of clay modifications and compatibilizers on the formation and physical properties of melt-mixed polypropylene/clay nanocomposites. Polymer Science, 42, 4139-4150.

[12] Modesti, M., Lorenzetti, A., Bon, D., and Besco, S., (2006) Thermal behaviour of compatibilised polypropylene nanocomposite: Effect of processing conditions. Polymer Degradation and Stability, 91, 672.

[13] Százdi, L., Pukánszky, B., Jr, Vancso, G. J., and Pukánszky, B. (2006) Quantitative estimation of the reinforcing effect of layered silicates in PP nanocomposites. Polymer, 47, 4638-4648.

[14] Suprakas, R., and Masami, O. (2003) Polymer/layered silicate nanocomposites: a review from preparation to processing. Progress in Polymer Science, 28, 1539-1641.

[15] Di, Y., Lannac, S., Sanguigno, L., and Nicolais L. (2005) Barrier and mechanical properties of poly(caprolactone)/organoclay nanocomposites. Macromolecular symposia, 228, 115-124.

[16] Wang, Y., Easteal, A.J., and Chen, X.D. (1998) Ethylene and oxygen permeability through polyethylene packaging films. Packaging Technology and Science, 11, 169-178.